ATME College of Engineering

18EE8732:Micro and Nano Scale Sensors and Transducers

MODULE – 3: Moisture Sensors
Optoelectronic and Photonic Sensors:

Prepared By,
Shreeshayana R
Electrical and Electronics Engineering
ATME College of Engineering, Mysuru

CONTENTS

3 A)Moisture Sensors: Structure, Theory, Main Experimental Results, Auxiliary Experimental Results

3 B) Optoelectronic and Photonic Sensors: Optoelectronic Microphone, Other Optoelectronic and Photonic Micro Sensors.

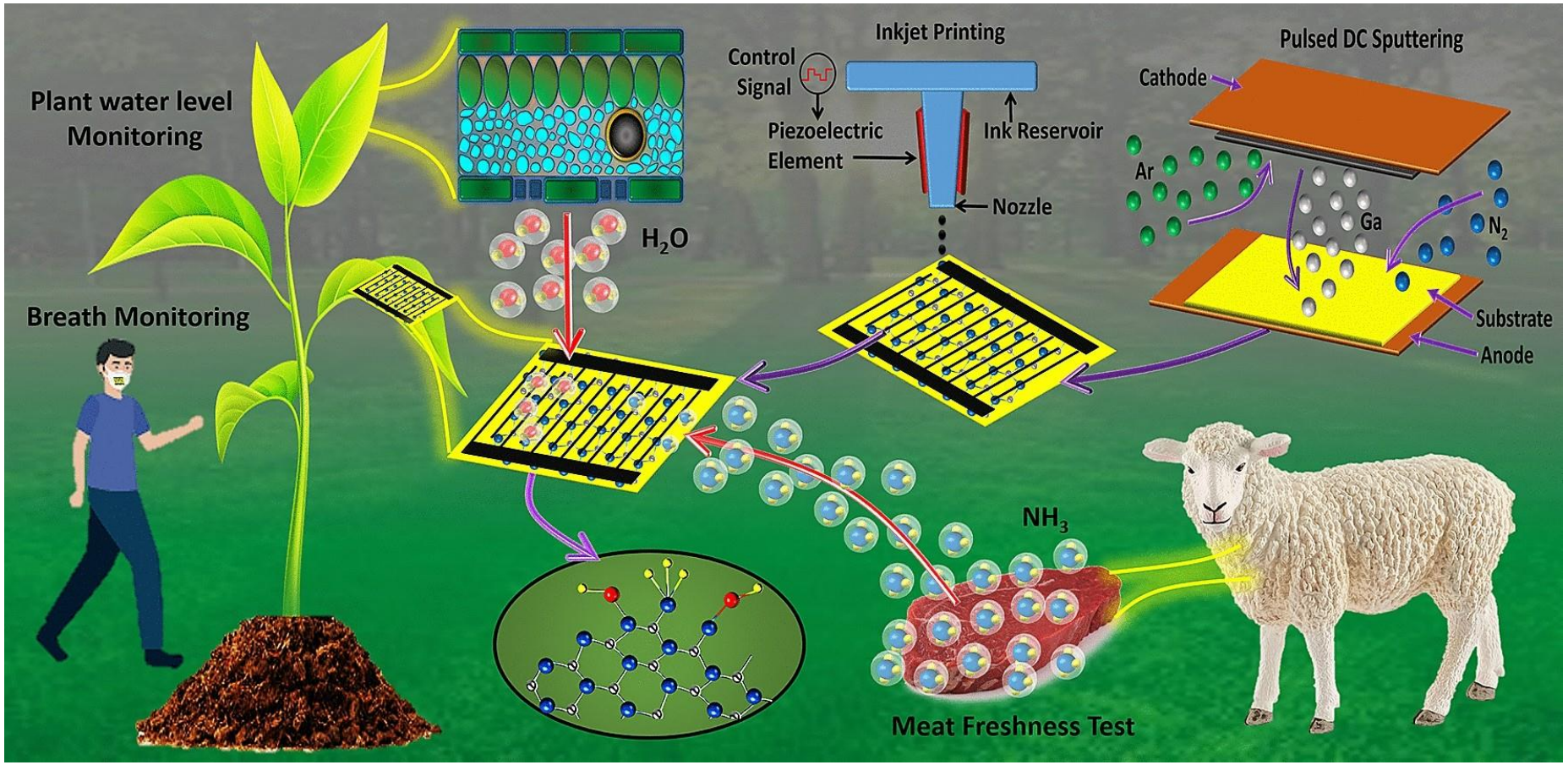
Plant water level Monitoring
Breath Monitoring
H_2O
Inkjet Printing
Control Signal
Piezoelectric Element
Ink Reservoir
Nozzle
Pulsed DC Sputtering
Cathode
Ar
Ga
N_2
Substrate
Anode
NH_3
Meat Freshness Test

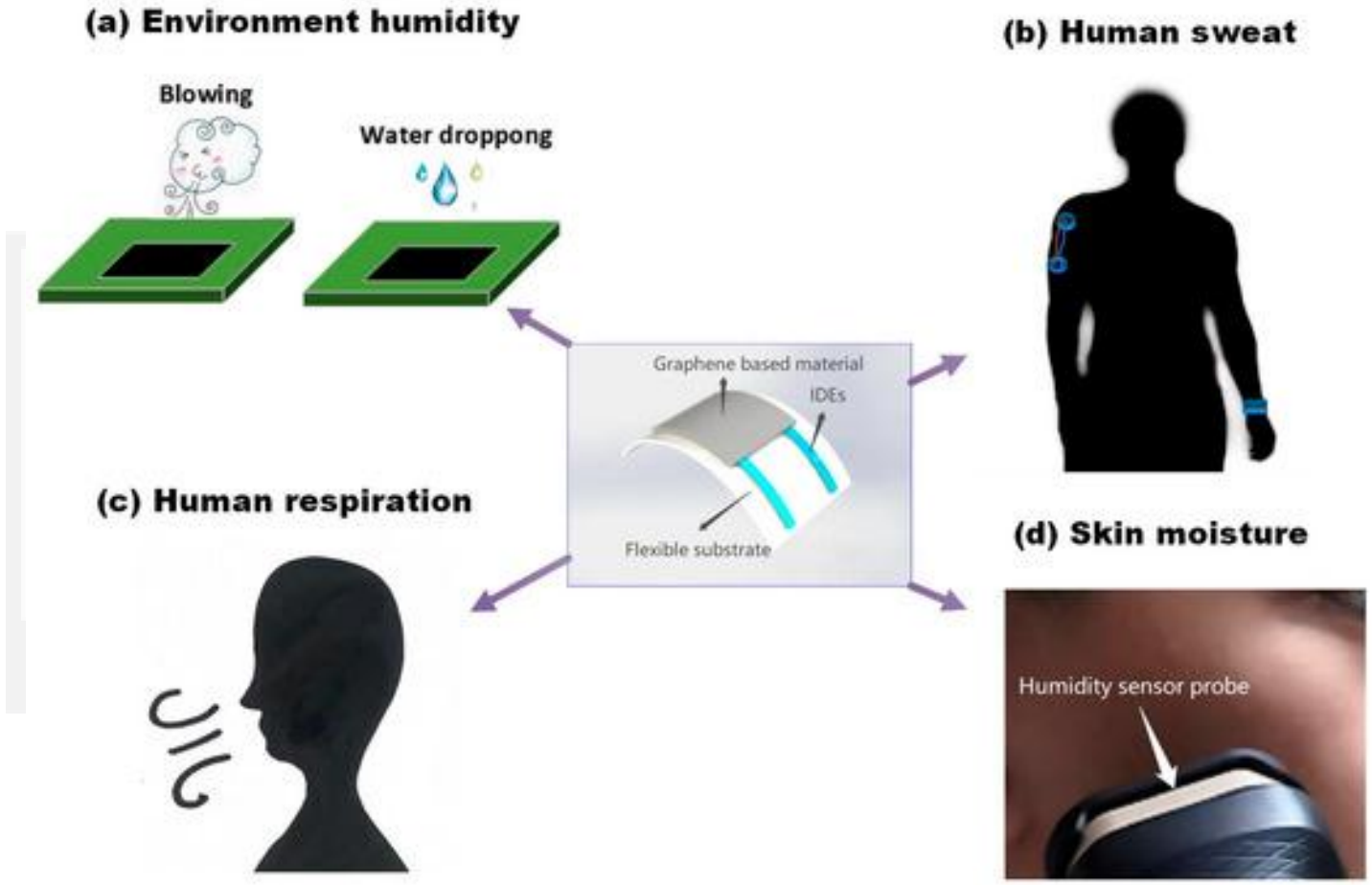
(a) Environment humidity
Blowing
Water droppong
(b) Human sweat
Graphene based material
IDEs
Flexible substrate
(c) Human respiration
(d) Skin moisture
Humidity sensor probe

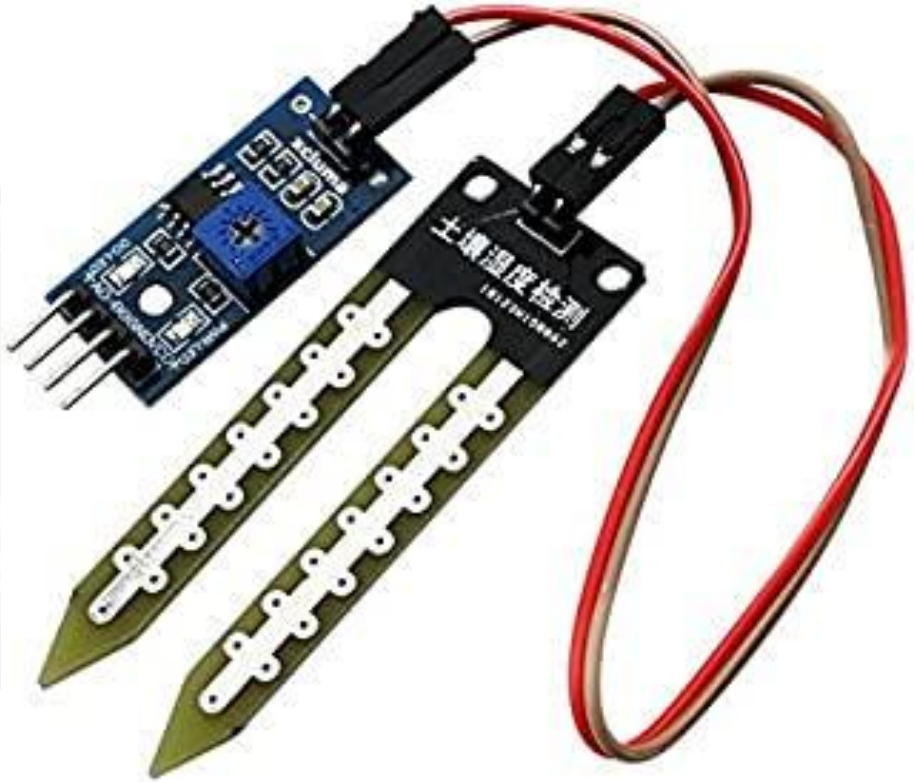
土壤湿度检测


SUNLIGHT
MOISTURE
pH
MOIST
pH
LIGHT
FRESHDCART

- Soil moisture sensors are used in numerous research applications,

E.g. agricultural science and horticulture including irrigation planning,

- Climate research,
- Environmental science including solute transport studies and
- Auxiliary sensors for soil respiration measurements.

- Soil moisture sensors are used for **measuring the water content of soil**. Multiple soil moisture sensors are combined to form a soil **moisture probe**.

- **Frequency domain sensors such as a capacitance sensor** is the most common sensor that is being widely used for commercial purposes.

Examples of various soil moisture sensors:
(A,B) **Capacitance sensors**;

(C) Tensiometer with an electronic gauge;

(D) Tensiometers with electronic gauges installed in a lettuce field and interfaced with a data-logger and radio communications;

(E) Tensiometer integrated with pressure transducer, data-logger

Tensiometers **measure soil moisture in units of negative pressure**, also known as tension.

Tension is a measure of the force that plant roots must exert to pull water from soil pores

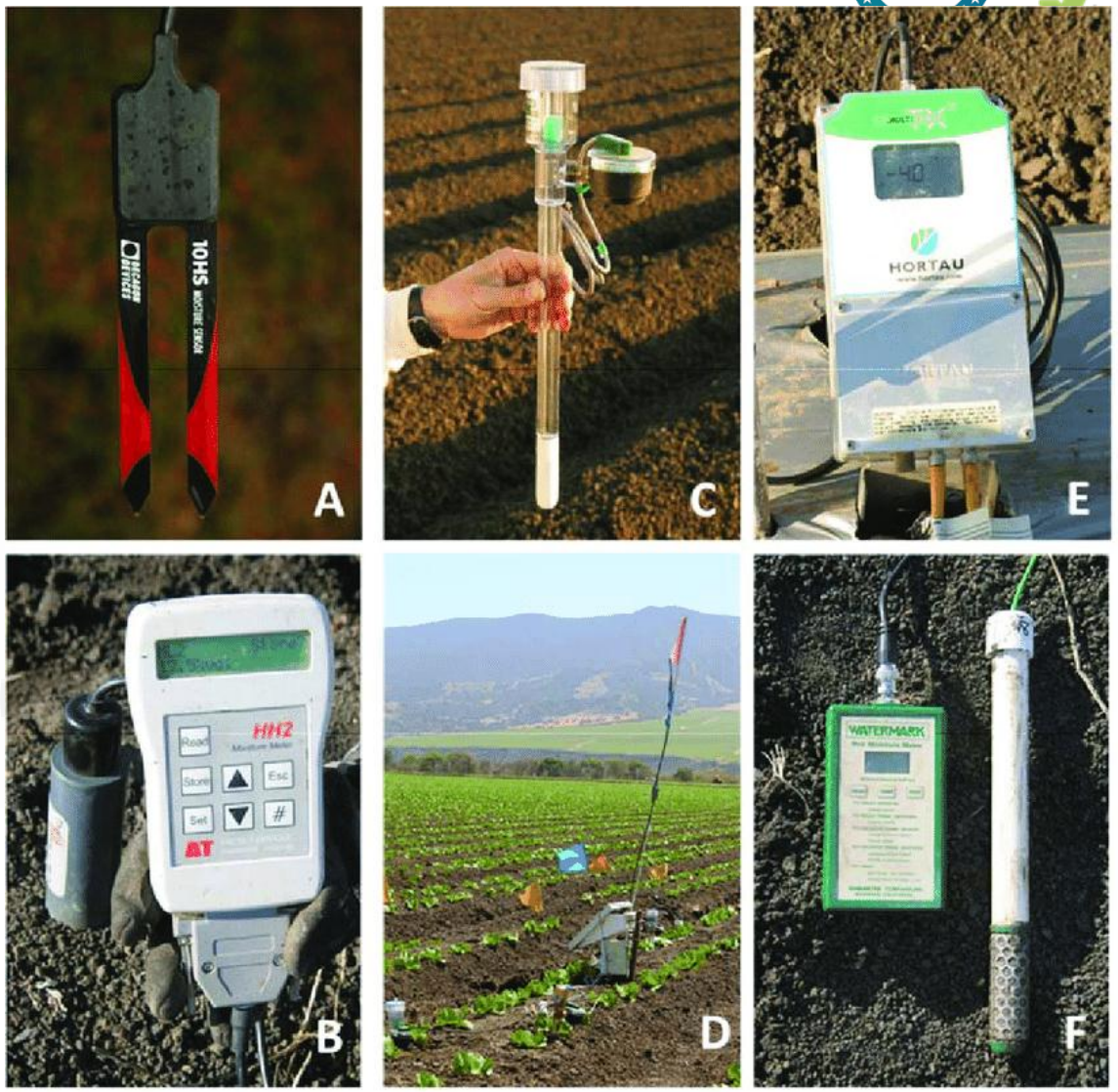

Moisture sensors exist in a number of varieties:

- Capacitive,
- Resistive,
- Microwave based, in addition to other more sophisticated varieties

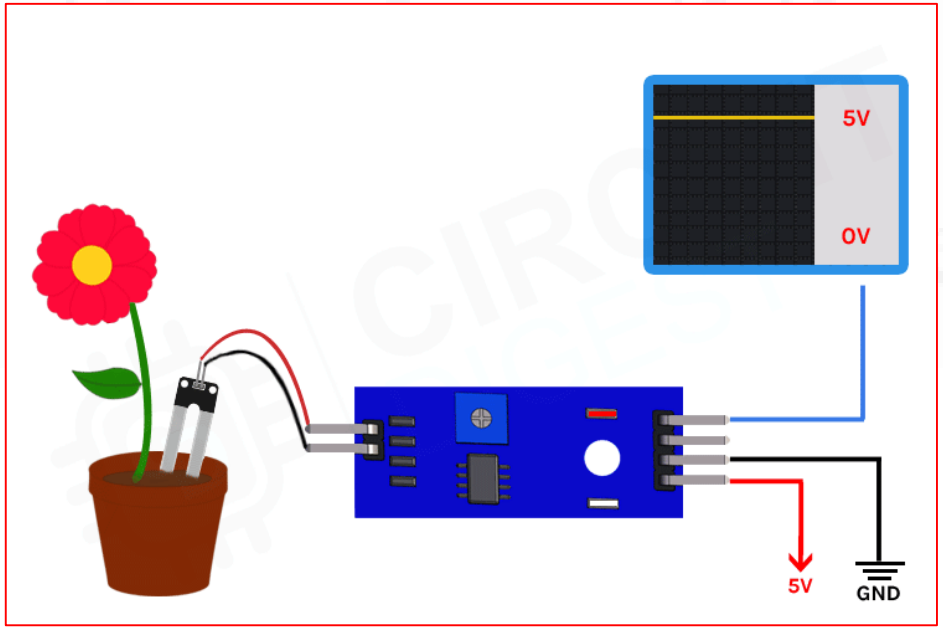

Among the technologies used at present, the **variable capacitance**- based moisture sensor is particularly noteworthy because of its **low cost** and the **simplicity of its design**

Drawback :variable capacitor used must be considerably large in order to obtain sufficient **sensitivity** to the **presence of moisture**

This limits the range of applications for this type of sensor.

This section Introduces a **new ultra-miniature, ultrahigh sensitivity moisture sensor** that is based on ultra-capacitor technology (a direct nanotechnology application)

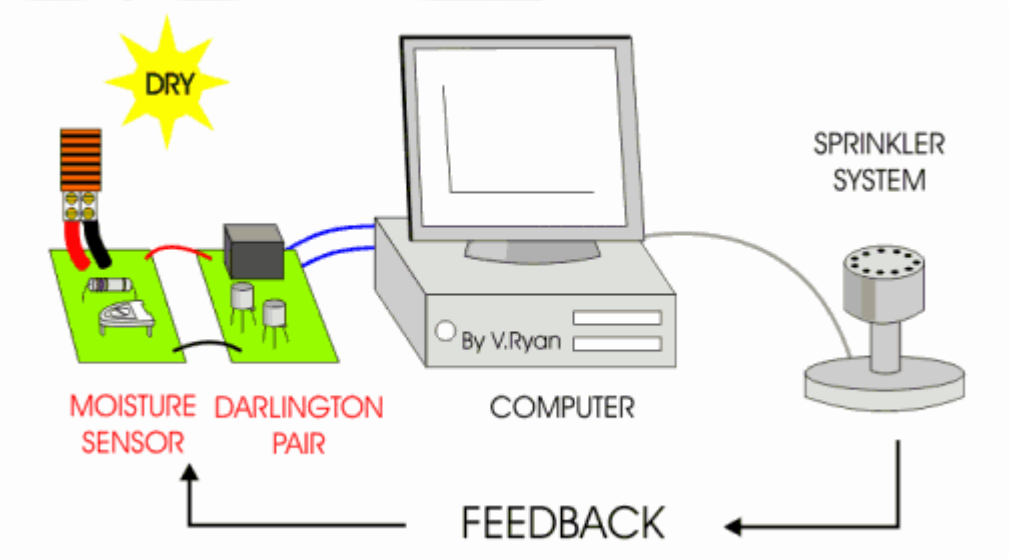

Structure

Step-1: The new moisture sensor is based on the idea of **using an ultra-capacitor structure** rather than an ordinary capacitor.

Inside the ultra-capacitor, **the moisture itself constitutes the electrolyte** that is needed for charge transfer

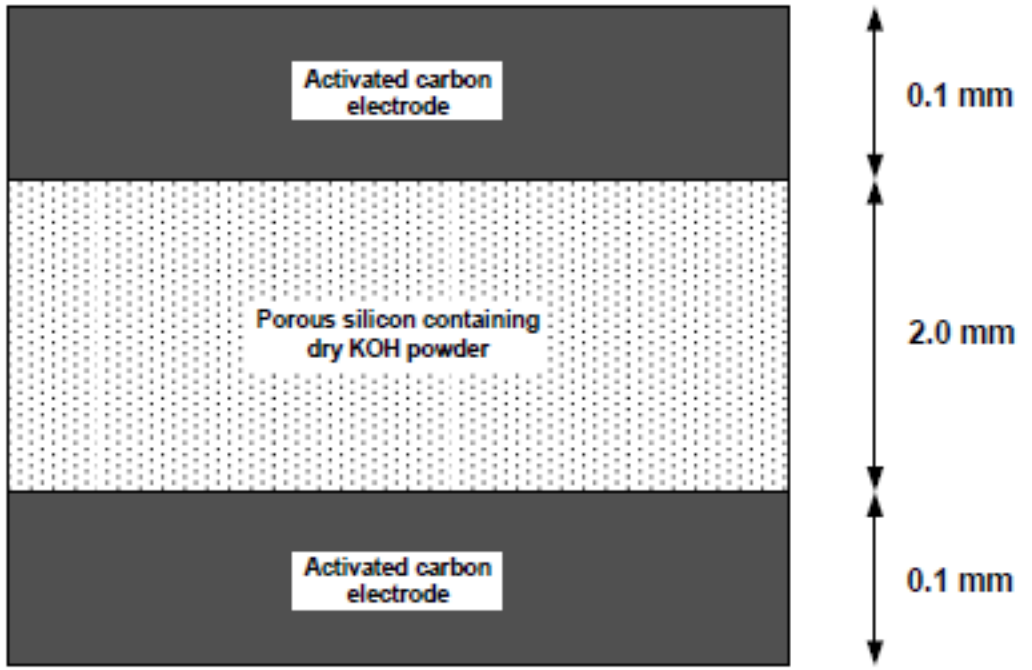

Structure

(a) An ultra-capacitor is assembled by using **two activated carbon electrodes** and an insulating layer of porous silicon.

Inside the pores of the silicon layer, **KOH (potassium hydroxide) in powder form is embedded.**

When the assembly is dry, no electrolyte exists inside the ultra-capacitor and hence the **capacitance of the device is equal to zero**

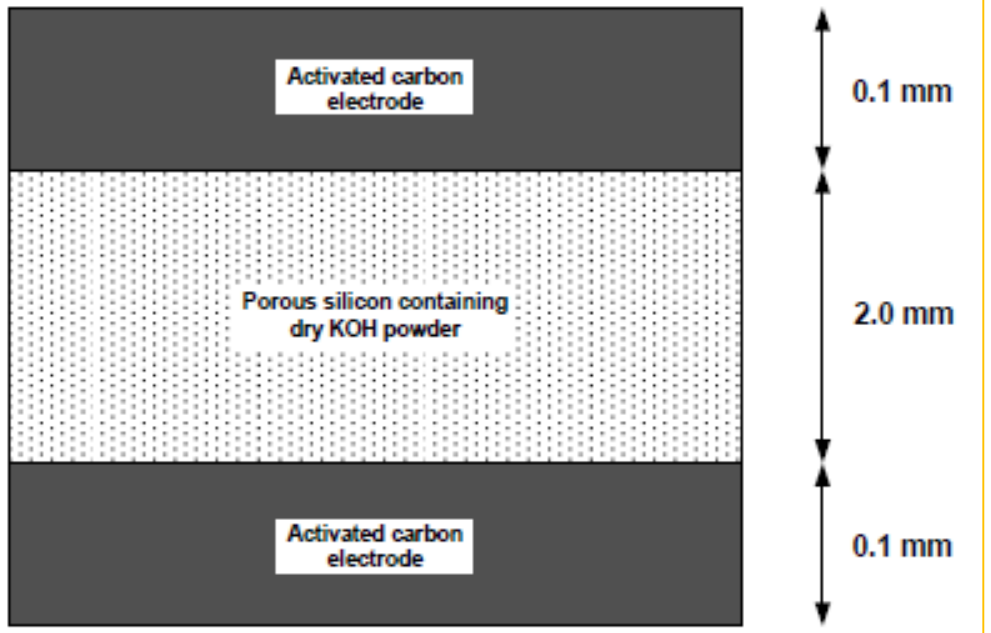

(a)

(b) In the **presence of moisture**, the combination of **KOH and water becomes an aqueous electrolyte for the ultra-capacitor**. The conductivity of the electrolyte and hence the **capacitance of the device increase as the moisture content increases.**

In the present prototype, the capacitance varies from **0 to approximately 17 µF** as the relative humidity is increased from **5% to 80%.**

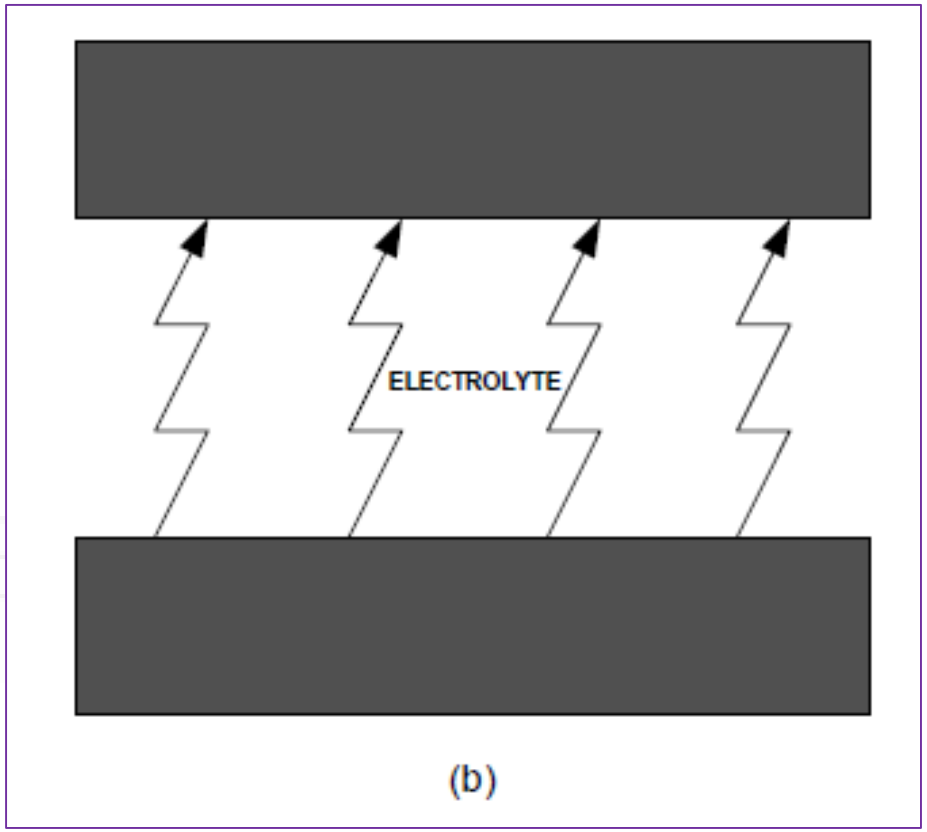

Structure

Step-2: This new sensor, however, has the highest sensitivity with respect to size among all known types of moisture sensors (including capacitive, microwave, and other sensors).

Applications:
Detection of moisture inside composite aircraft materials, and other embedded moisture sensing applications where high sensitivity and a miniature size are desirable

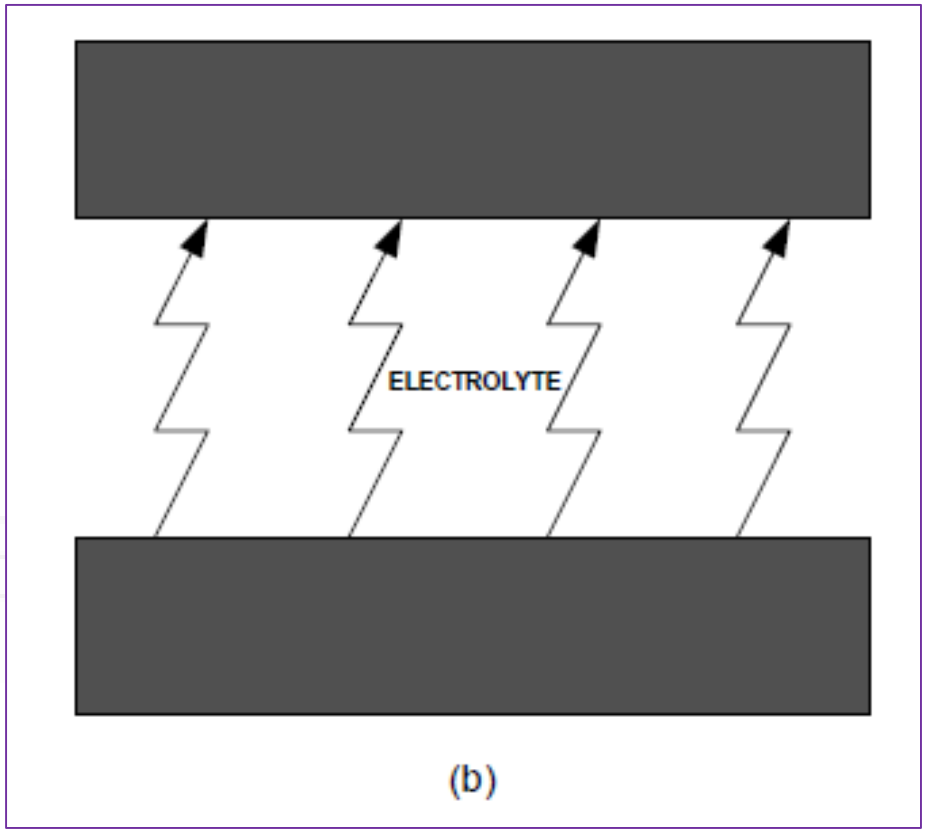

Step-3: The prototype shown in the figure measures 8 mm × 8 mm and its total thickness is approximately 2 mm. The sensor can be made much smaller.
A 2 mm × 2 mm sensor exhibits a total capacitance variation of **about 1 µF**

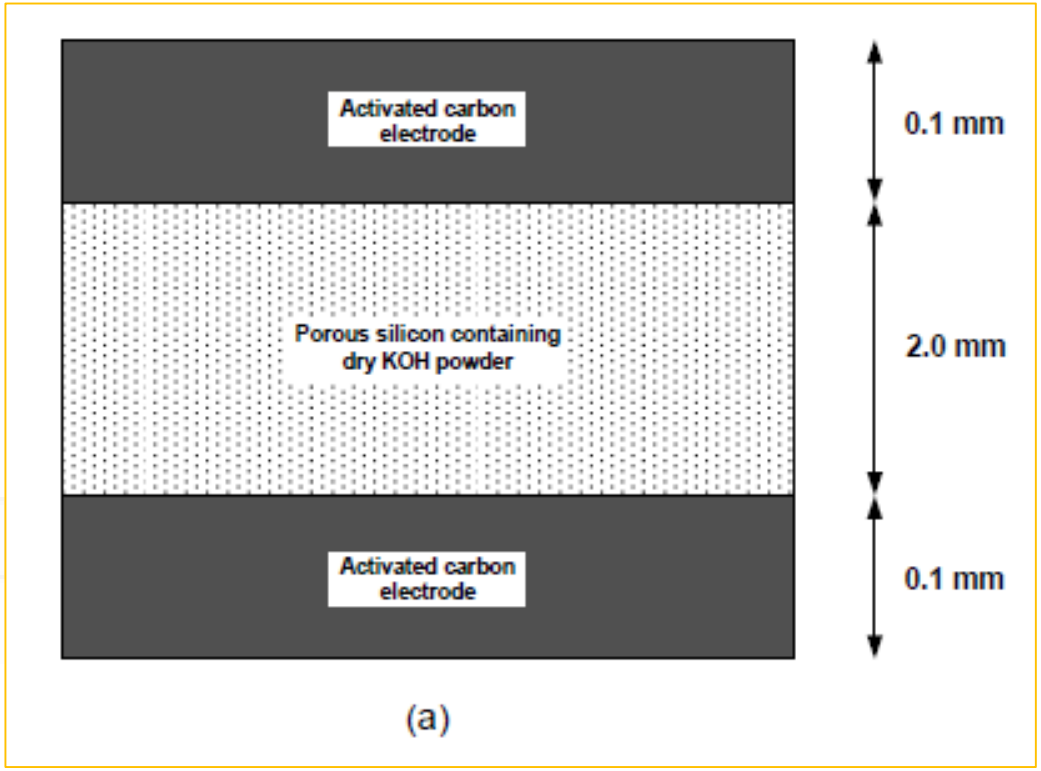

Step-4: The activated carbon electrodes do not occupy the entire surface area of the porous silicon slab, in order to allow moisture to seep through the pores of the slab.

Step-6: The activated carbon electrodes were deposited with **screen printing**, and the thickness of each electrode is approximately **0.1 mm**.

The electrodes deposited with this technique have an internal surface area of approximately 500 m^2 per gram of the material

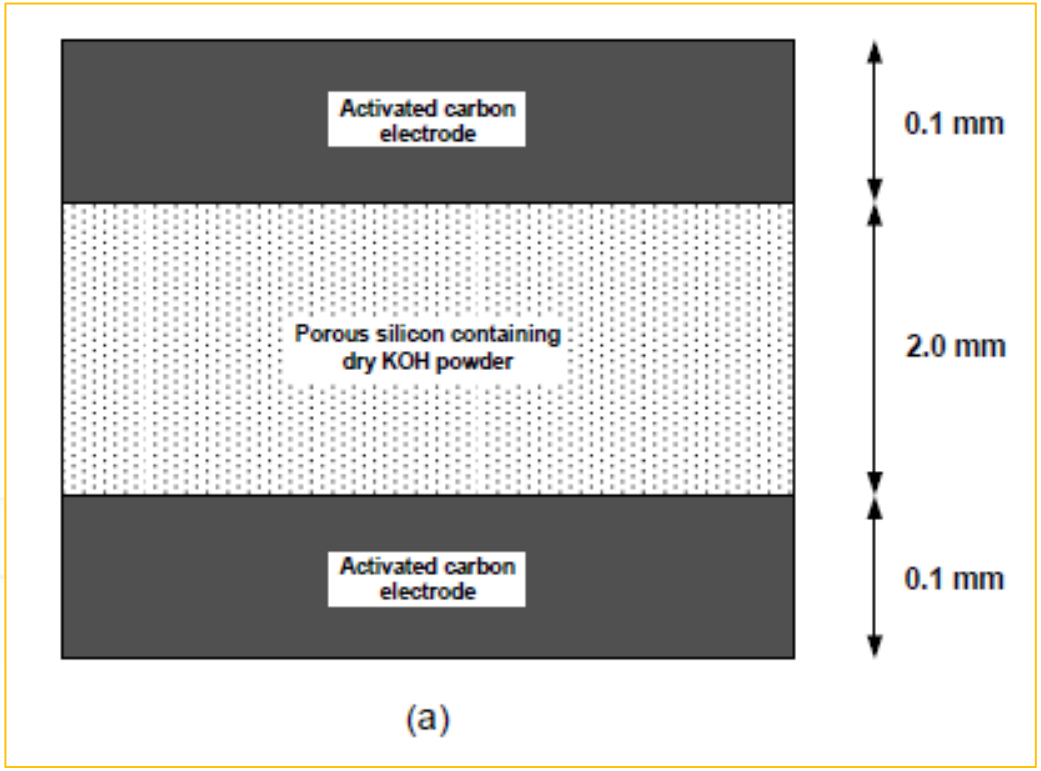

(a)

Step-7: The mean pore size (diameter) of the pores in the slab is **approximately 10 nm**. To embed the KOH powder inside the slab, **KOH at a concentration of 35%by weight** was first dissolved in distilled water, and the slab was soaked in the solution.

The slab was then sintered in a furnace at a temperature of **500◦C for 30 min to remove the water**.

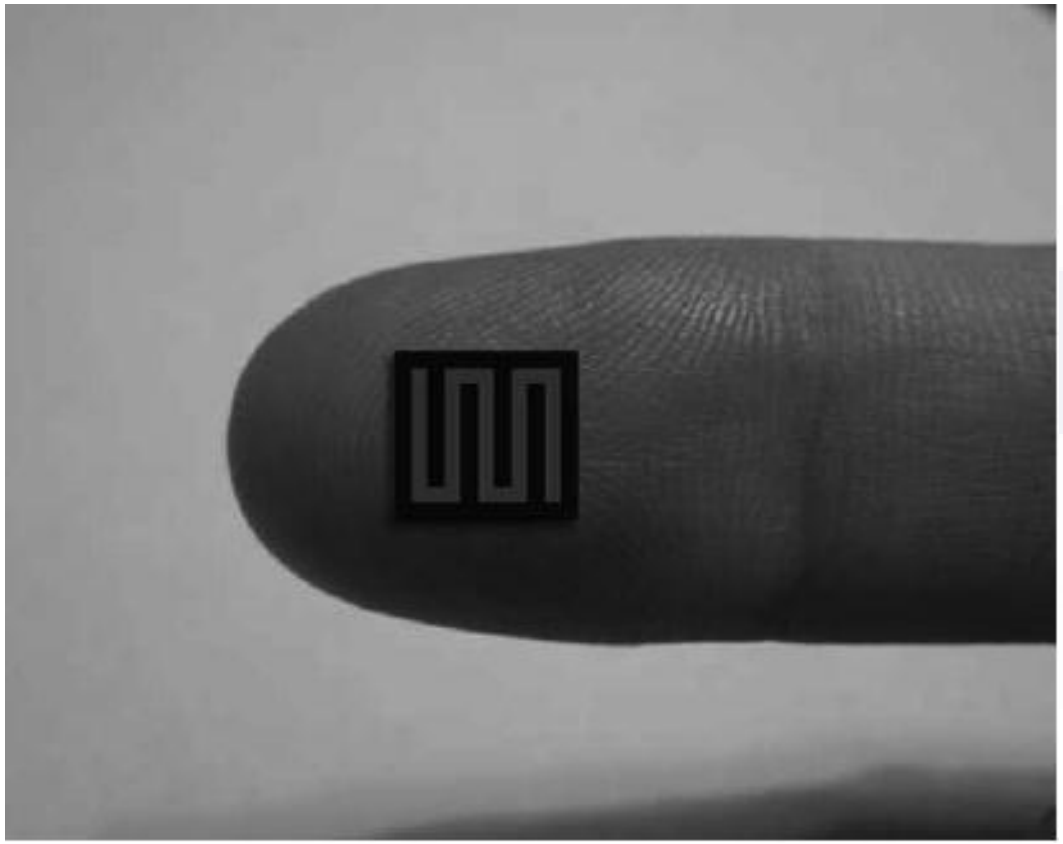

Photograph of the sensor, resting on the author's finger. The sensor measures 8 mm × 8 mm.

Theory

The **objective** is to obtain a mathematical relationship between the **capacitance of the ultra-capacitor** and **the conductivity** of the electrolyte inside the device

The **current density *J*** in any medium is related to the **conductivity *σ*** by the following well-known equation

$$J = \sigma E$$

where ***E* is the electric field intensity**.

J and E are further related to the current I and the voltage V by the relations

$$J = \frac{I}{A} \qquad E = \frac{V}{d}$$

where ***A* in the present application is the cross-sectional area of the porous slab** and

***d* is its thickness.**

Hence,

$$\frac{I}{A} = \sigma \frac{V}{d}$$

The current through the electrolyte will be related to the rate of flow of charges by

$$I = \frac{dQ}{dt}$$

where Q is the ionic charge moving through the cross-sectional area of the slab

From the previous two equations, we have

$$\frac{dQ}{dt} = \frac{AV}{d}\sigma(t)$$

In the above equation, the **conductivity is assumed** to be a **time-varying quantity** (the conductivity will be indeed slowly varying as moisture seeps through the device),

Voltage *V* across the terminals of the ultra-capacitor is assumed to be constant

$$Q = \frac{AV}{d}\int \sigma(t)dt$$

The **accumulated charge *Q* at each of the two interfaces** in the ultra-capacitor is related to the capacitance of the interface by the well-known relationship

$$Q = C_{int} V_{int}$$

where C_{int} is the capacitance of the interface and V_{int} is the voltage across the interface.

$V_{int} = V/2$, where V is the total voltage applied to the device

From

$$Q = \frac{AV}{d}\int \sigma(t)dt$$

$$Q = C_{int}V_{int}$$

$$\frac{1}{2}C_{int}V = \frac{AV}{d}\int \sigma(t)dt$$

$$C_{int} = \frac{2A}{d}\int \sigma(t)dt$$

But the total capacitance C is equal to $C_{int}/2$ (since the configuration is essentially that of two capacitors in series)

$$C = \frac{A}{d}\int \sigma(t)dt$$

integral of σ over time is dimensionally equivalent to the permittivity $\in$ of a medium

Main Experimental Results

The sensor was tested in a computer-controlled chamber that features variable humidity and variable temperature

Figure shows the measured conductivity of the porous silicon slab at **25^{0}C**, as the relative humidity **was increased** from **5% to 80%.**

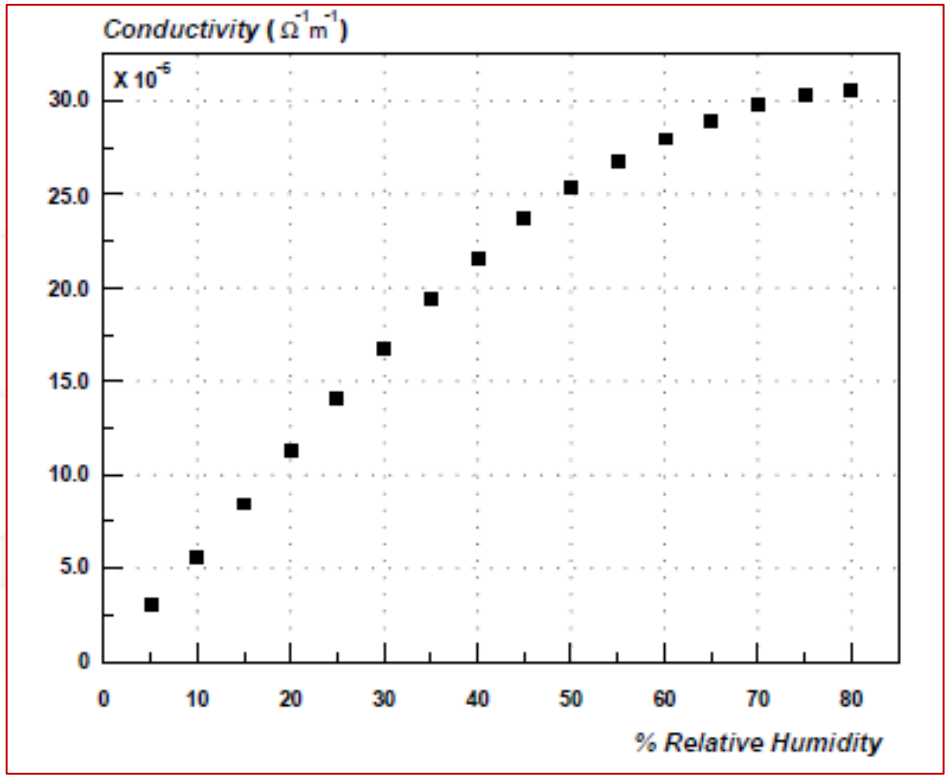

Main Experimental Results

Conductivity of the porous silicon slab at **10◦C** and **70◦C**, as the relative humidity is increased from **5% to 80%.**

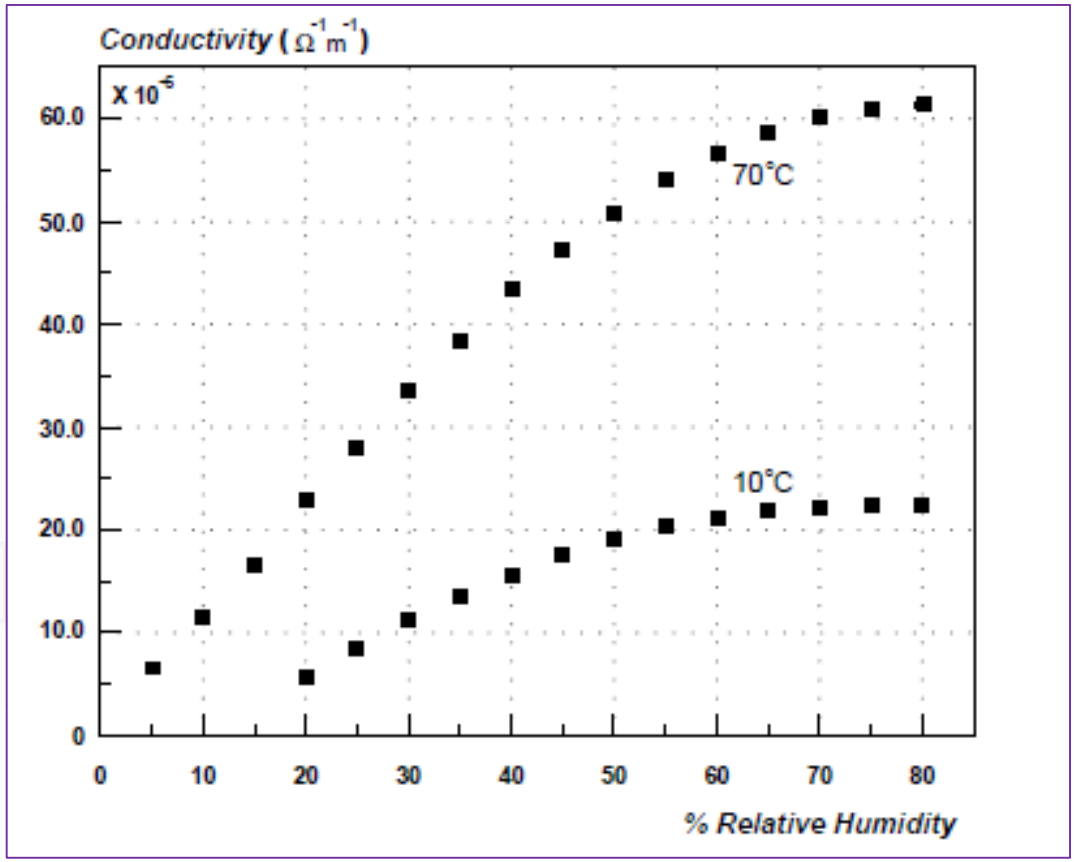

Observation :It should be pointed out that the fact that water solidifies at **0◦C and boils at 100◦C**, in combination with the fact that most humidity control chambers can reliably control the humidity in the range of **10 to 70◦C**, make this particular range of temperatures (10–70◦C) the most suitable range for testing a moisture sensor

Main Experimental Results

Figure shows the measured capacitance C of the sensor at **25◦C**, as the relative humidity was **increased from 5% to 80%.**

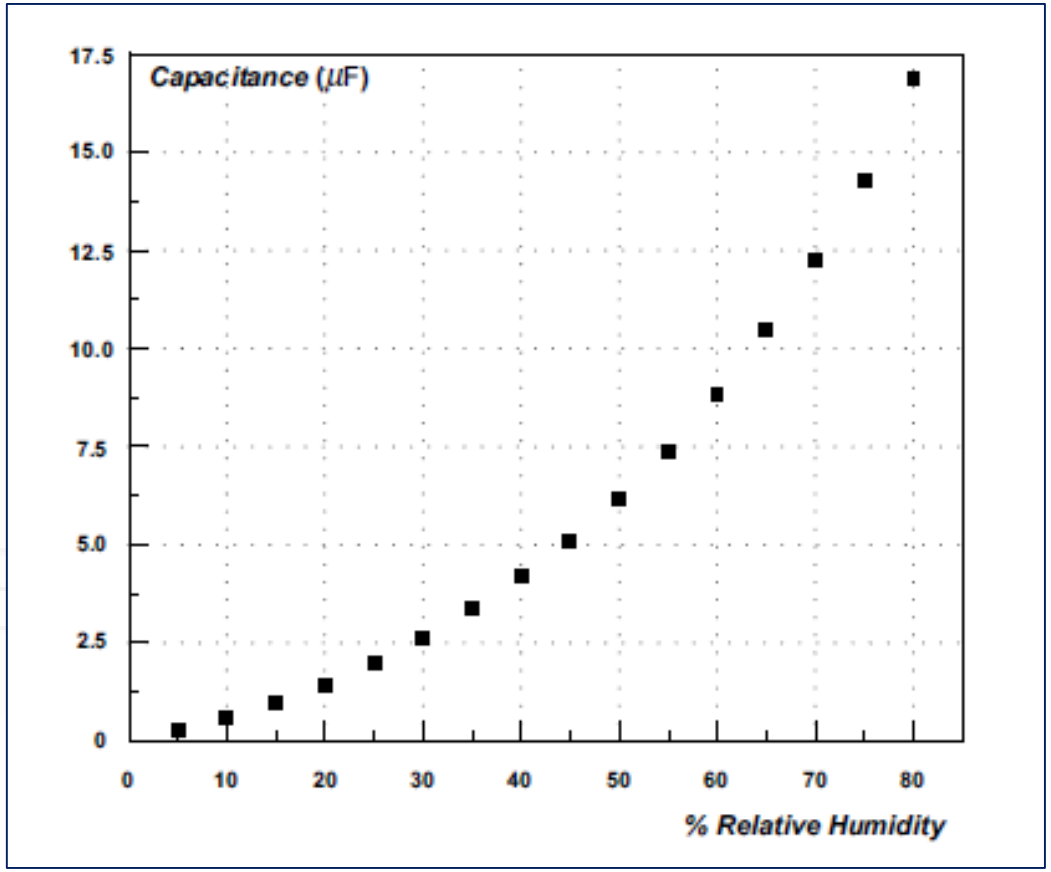

Main Experimental Results

Figure shows the same measurements, repeated at temperatures of **10◦C and 70◦C as the relative humidity is increased from 5% to 80%.**

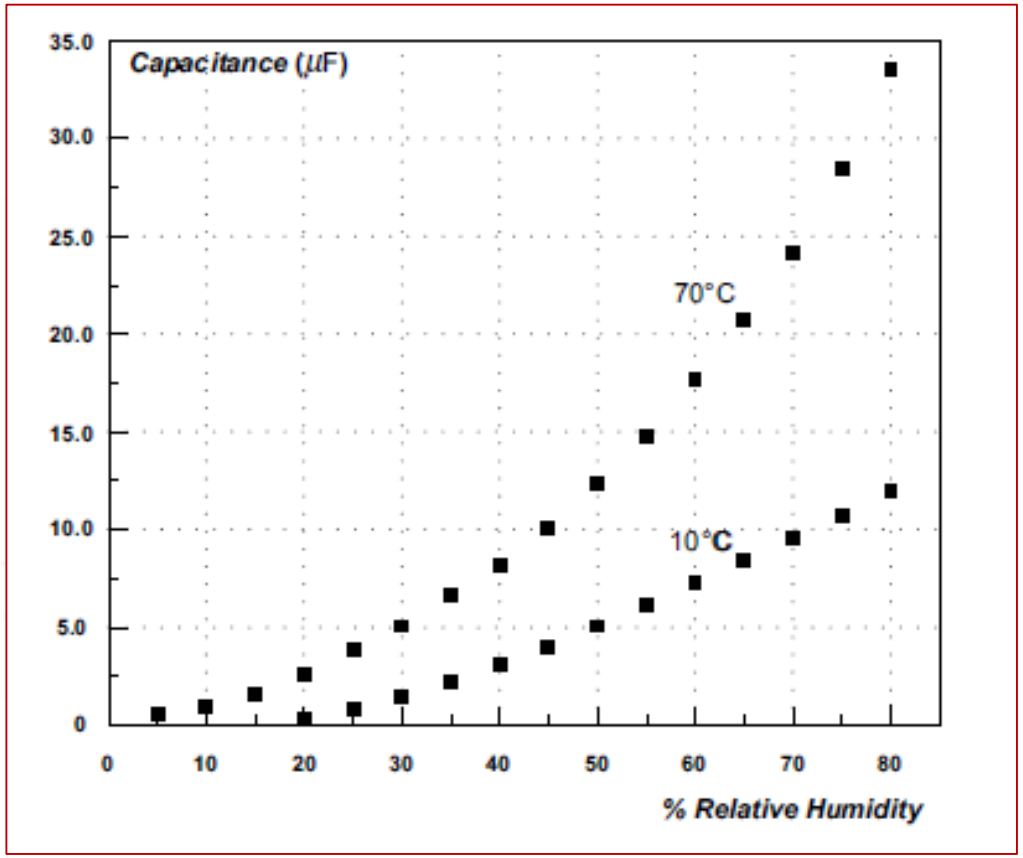

Main Experimental Results

Plots of the variation of the conductivity and capacitance as functions of time are shown in Figure , as the relative humidity is increased as a step-function from **5% to 10%.**

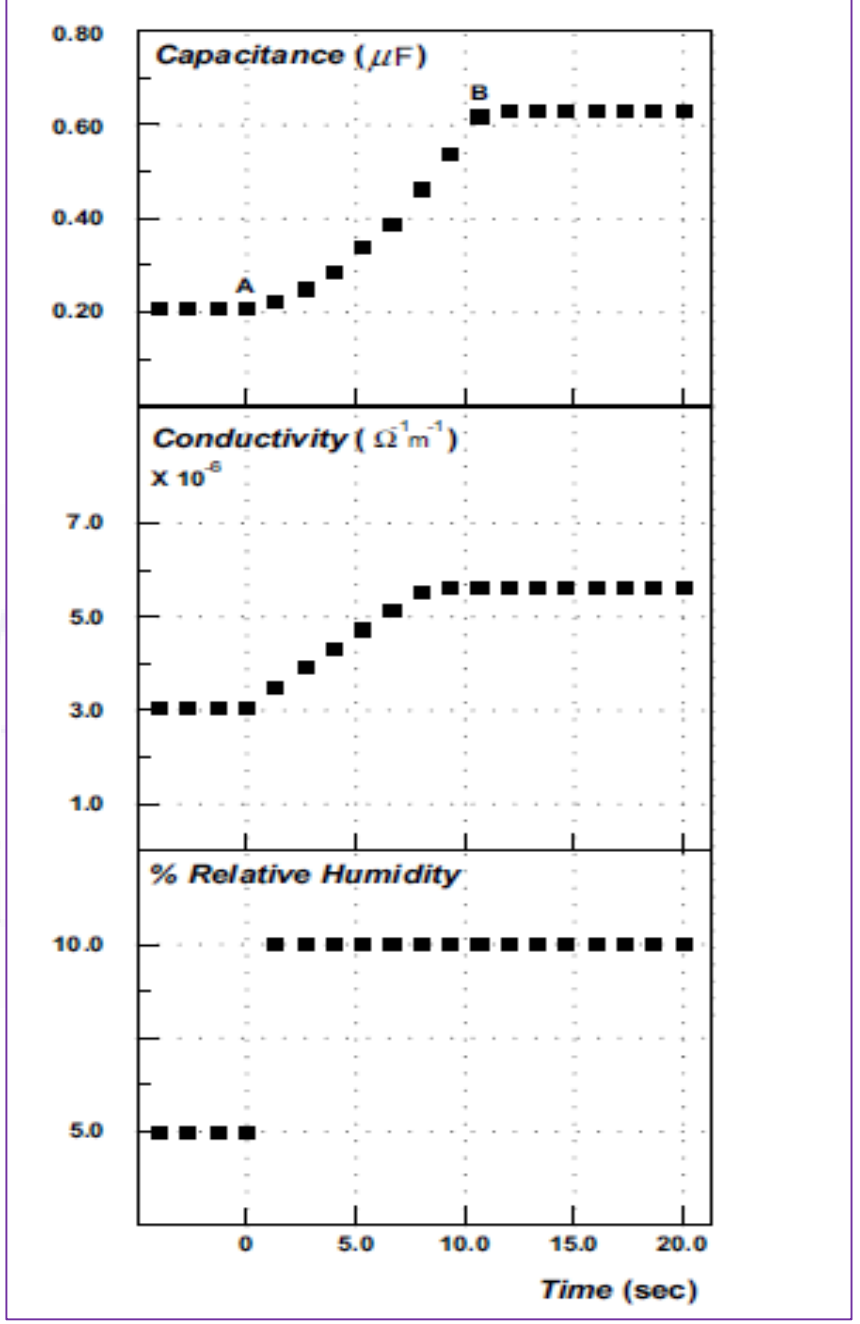

As the plots show, s increases linearly from approximately $3\times10^{-6}\,W^{-1}m^{-1}$ to $5.6\times10^{-6}\,W^{-1}m^{-1}$ where after it remains constant

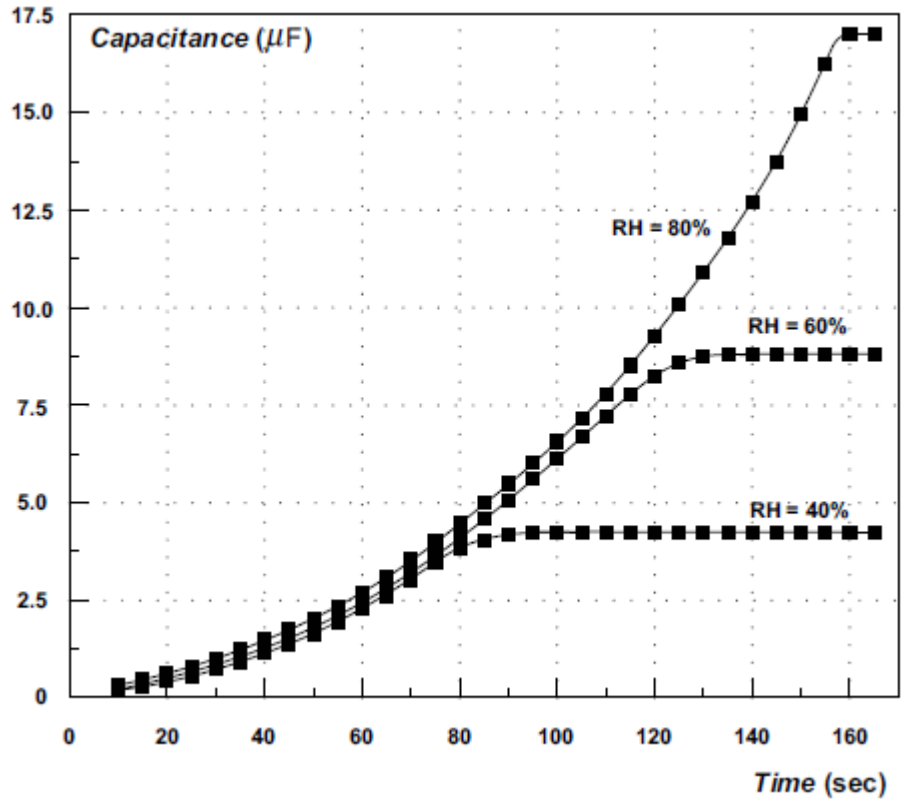

Capacitance actually stabilizes at a constant value of about 0.63 μF

The reason for this deviation from the expected behavior is the following:

a) the **porous silicon slab** is a complicated medium.

b) Due to the structure of the pores, certain paths within the slab become **conductive as the relative humidity is increased**, while other paths do not accumulate sufficient moisture to become conductive.

c)Once all the available charges within a conductive path migrate to the activated carbon electrodes, the path becomes **"saturated"** and no further migration of charges can occur. The capacitance therefore remains constant

Temperature hysteresis curves. The maximum hysteresis error in the measured capacitance of the sensor is approximately 12% FSO, as the temperature is cycled from 10◦C to 70◦C.

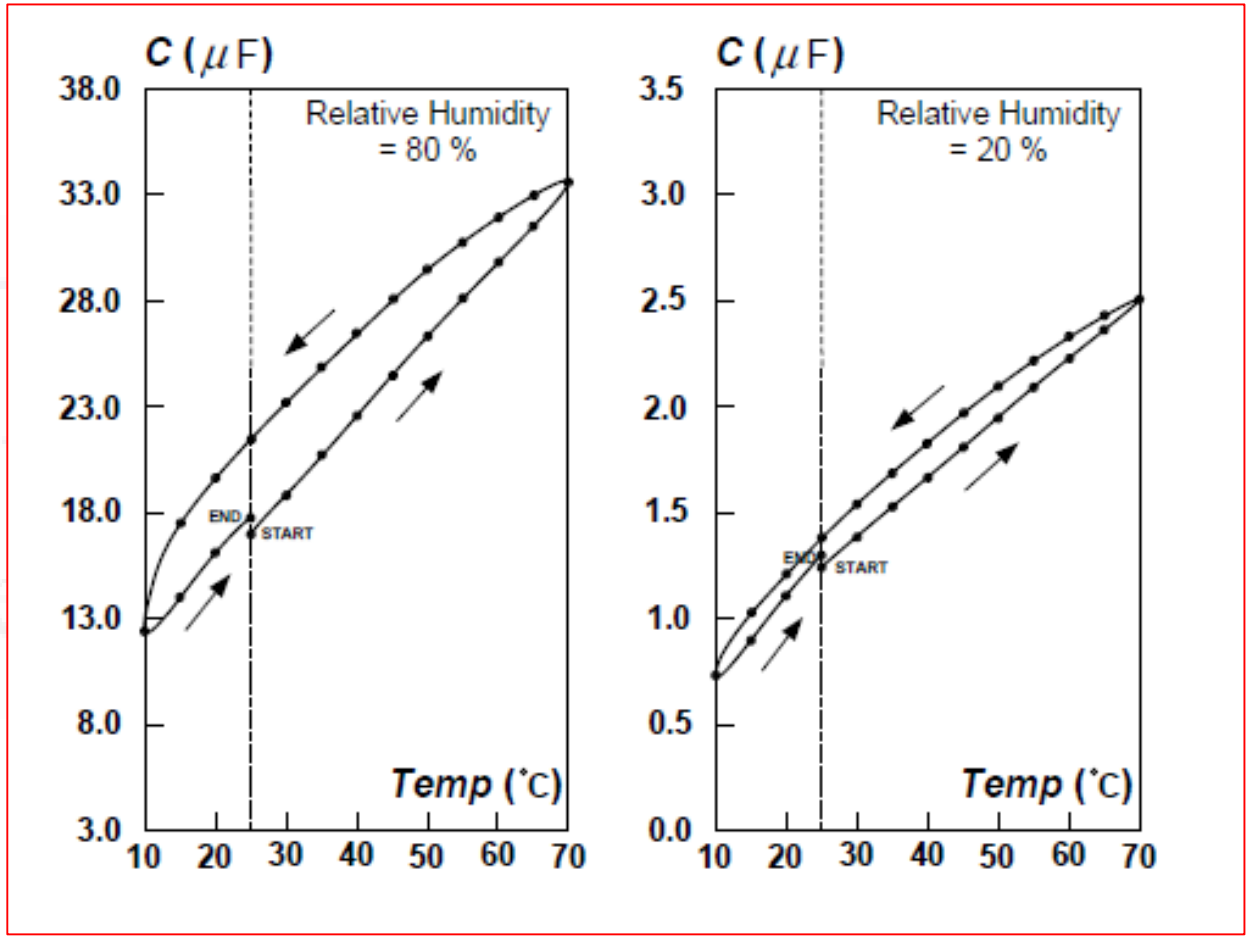

The circuit is a well-known 555 oscillator circuit that converts an unknown capacitance to frequency.

It is to be pointed out that the interface circuit does not amplify or compensate for the characteristics of the sensor.

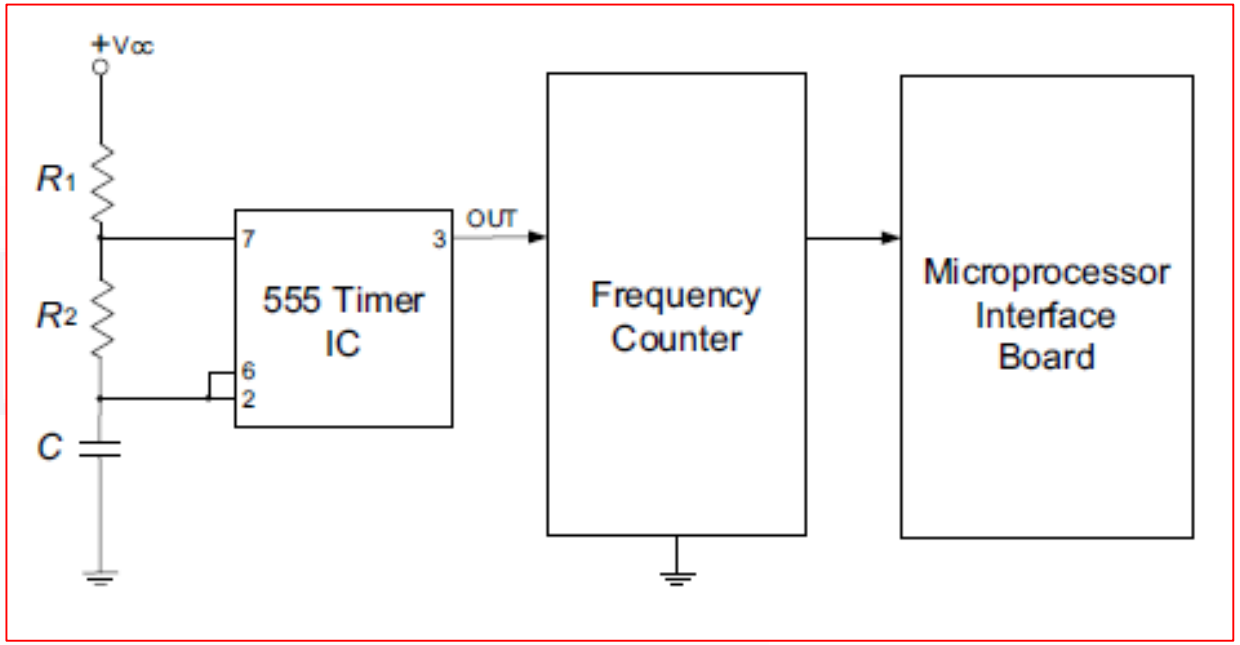

MODULE 3 B)

3 B) Optoelectronic and Photonic Sensors:

Optoelectronic Microphone, Other Optoelectronic and Photonic Micro Sensors.

Optoelectronic Microphone

Nanotechnology has revolutionized a number of classical applications by allowing the integration of **optical sensing techniques** into such applications

Advanced new products in this category include **optical microphones**, **fingerprint readers**, and **highly sensitive seismic sensors**.

The microphone uses a **charge-coupled device (CCD) as its sensing mechanism.**
This new type of microphone will be available commercially within a time span of 1 to 3 years.

Principle of Operation

Novel new optical microphone that is characterized by structural simplicity, low cost, very large **dynamic range, and excellent frequency response characteristics** was introduced.

A conventional, **thin metallic diaphragm** vibrates in response to sound pressure.

Principle of Operation

As shown in Figure (a), **a conventional, thin metallic diaphragm** vibrates in response to sound pressure

The diaphragm has a **reflective pattern** that is **etched on its surface** (the pattern used in the present prototype is a group of reflective circles).

A group of **light-emitting diodes (LEDs)** are arranged underneath the diaphragm, as shown, to illuminate the reflective pattern

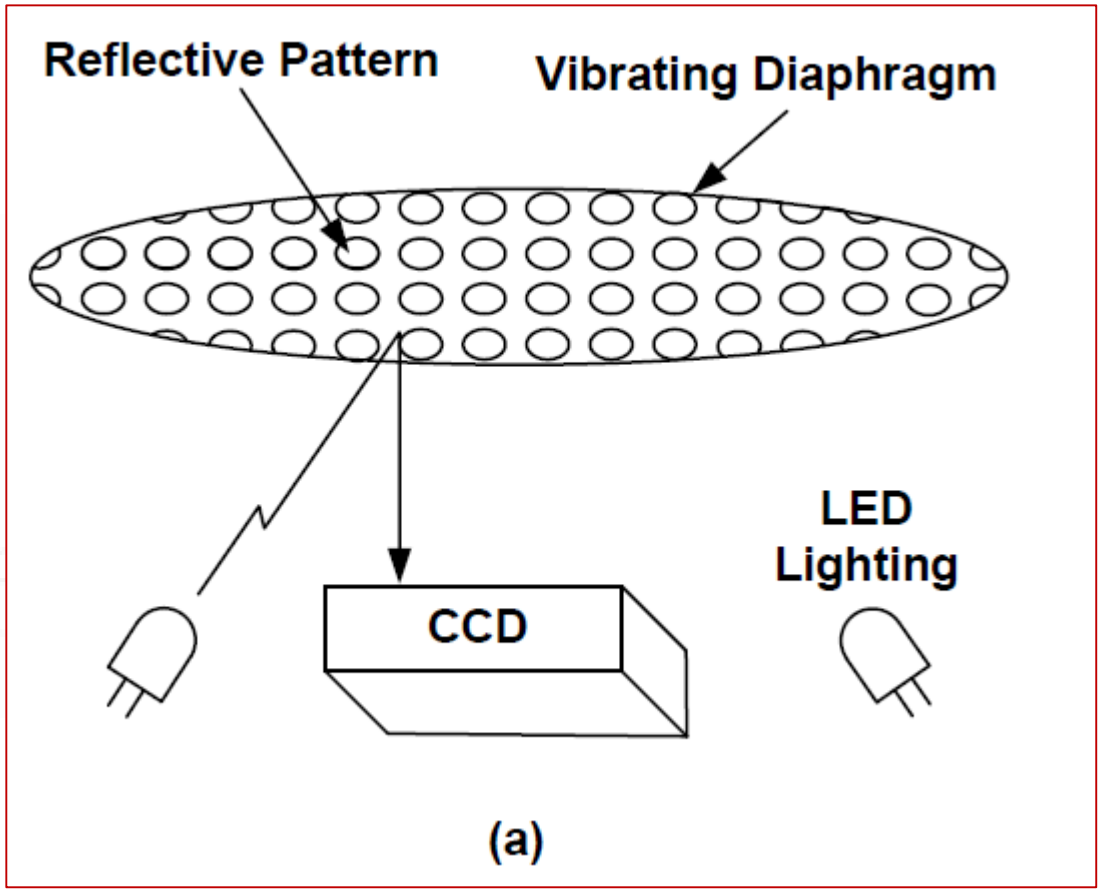

Principle of Operation

The image of the pattern is then captured by a CCD and is passed to a microprocessor for pattern recognition.

Hence, **pattern recognition is the distinctive new feature** in this type of microphone.

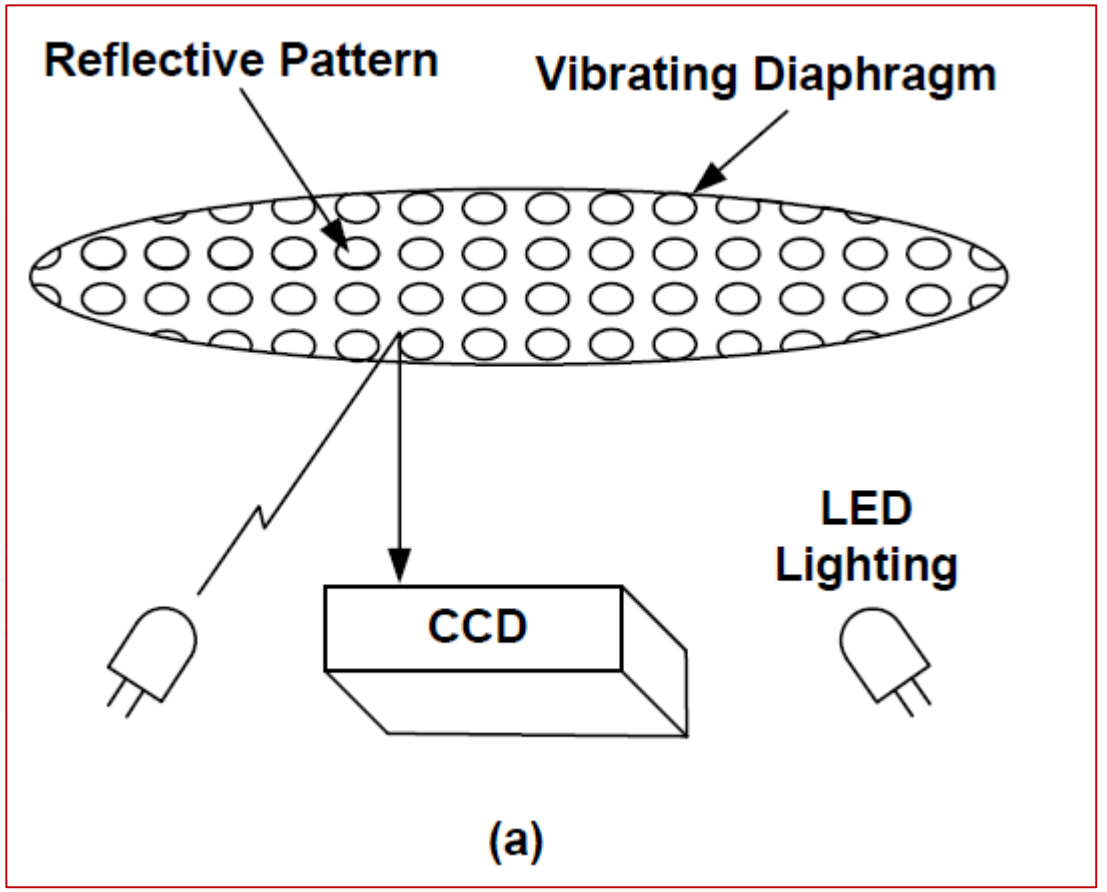

Principle of Operation

Figure (b) shows the typical picture of the pattern when the diaphragm is flexed away from the CCD

Figure (c) shows the perceived pattern when the diaphragm is flexed toward the CCD.

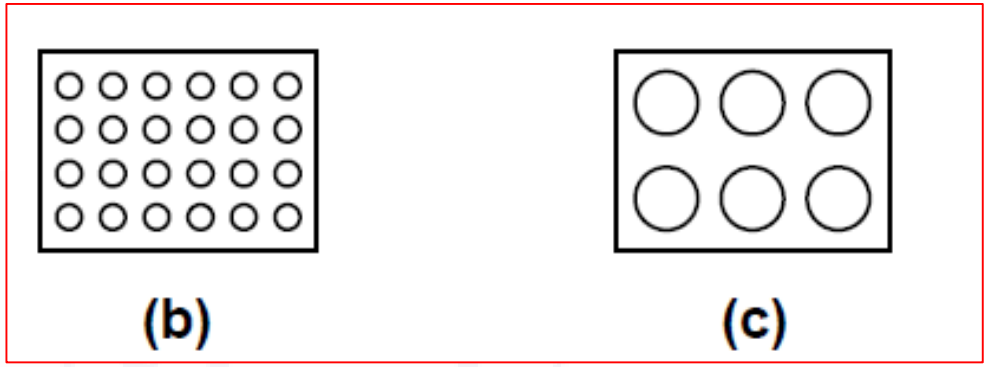

With the availability of **cheap, high speed electronics**, the CCD can be easily sampled at a rate of **32 to 40 kHz** and pattern recognition can be performed in real time to detect the instantaneous position of the vibrating diaphragm

Main components of the microphone:

- The patterned metallic diaphragm,
- The circular LED array,
- A wide-angle fixed-focus lens, and
- The CCD (mounted on its own interface board).

One US penny is shown in the photo for size comparison.

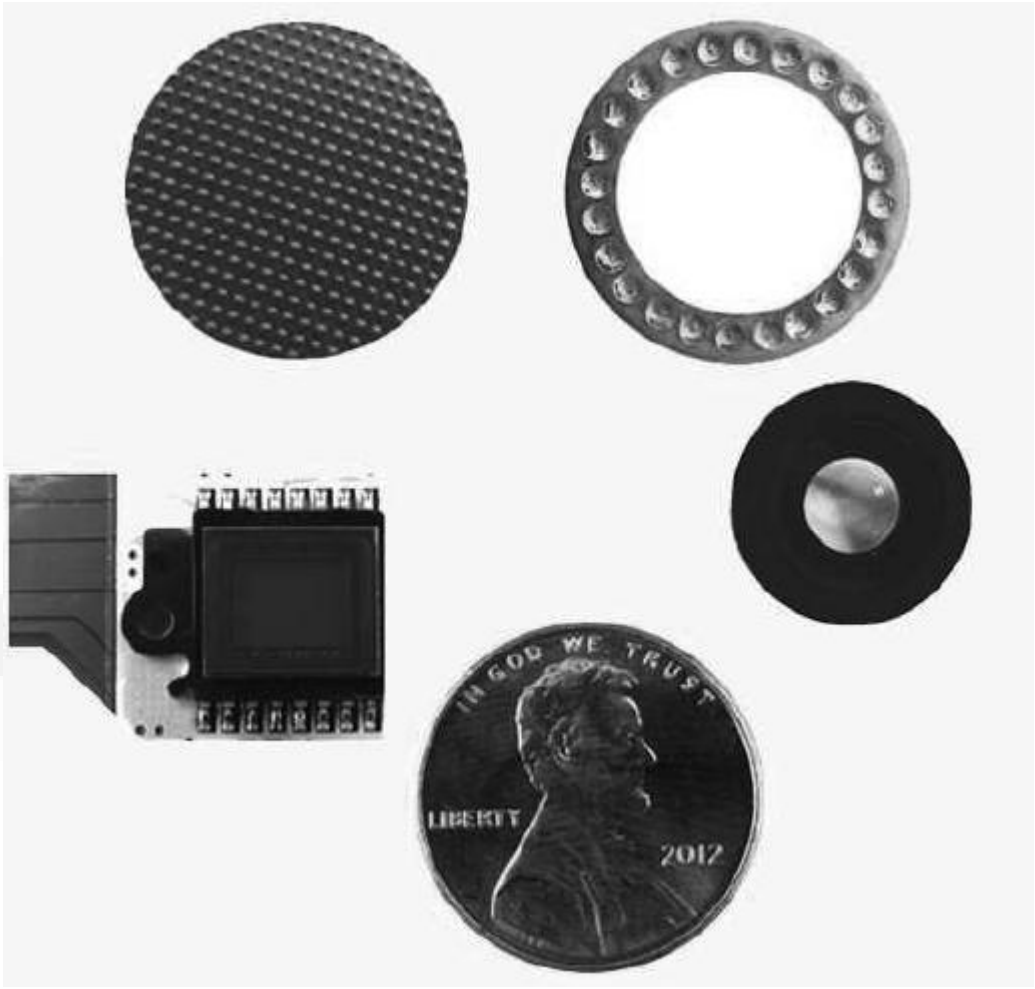

Mechanical diagram of the integrated microphone assembly

Figure is a mechanical diagram that shows how the components were assembled to form a fully **integrated microphone**.

- It is to be pointed out that the **wide-angle**, **fixed-focus lens** that is used in the prototype can keep the diaphragm's image focused on the **CCD even if the diaphragm moves** by as much as a few millimeters (in actual
- Micro-phony applications, movements of the diaphragm are typically on the order of nanometers or angstroms).

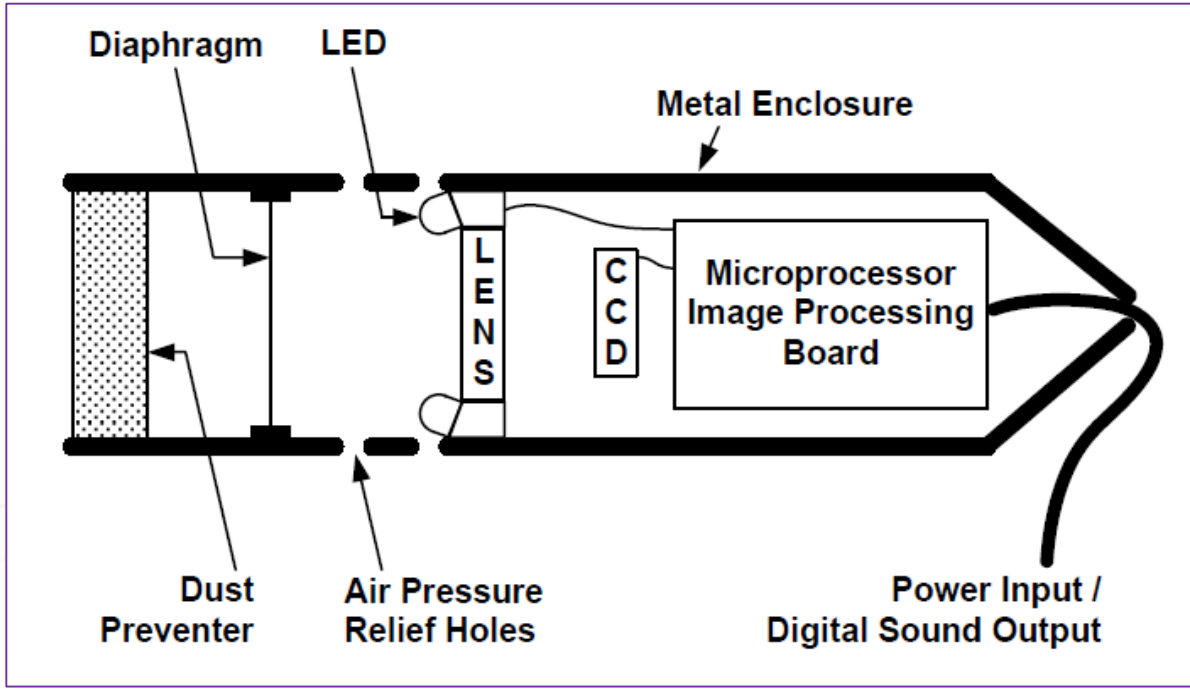

Mechanical diagram of the integrated microphone assembly

The CCD used in the present prototype is a low resolution (640 × 480 pixels) CCD that comes with the CMU CAM image processing board.

The CMU CAM is an **off-the-shelf miniature image processing board** that was chosen for the present prototype.

A number of custom-modified versions of the board are available commercially.
It is to be pointed out that an image subsample of only **32 × 32 pixels** is actually used in the present application due to timing constraints on the small, low-cost hardware that was chosen

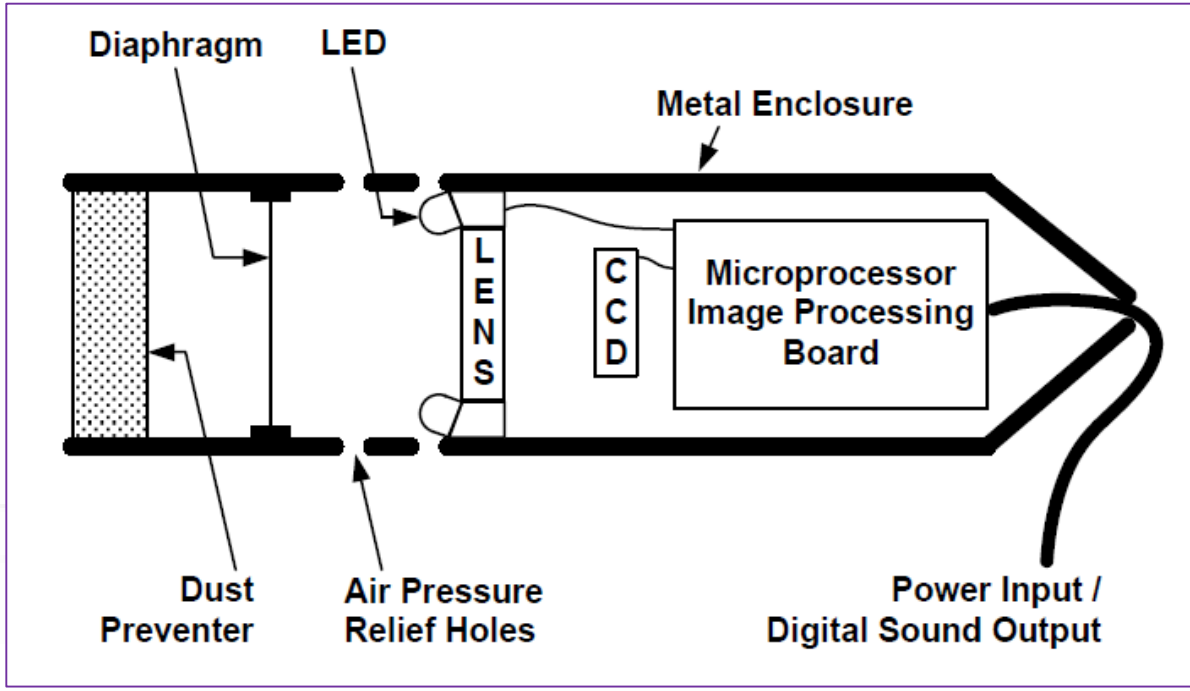

Mechanical diagram of the integrated microphone assembly

CCD is mounted on an interface board for row/column scanning, and the interface board connects to the microprocessor board with a flexible connector.

The LEDs that are used for illumination are miniature red LEDs, **as CCD devices are known to be most sensitive to red light**

However, **LEDs of any color can in principle be used in this application.**

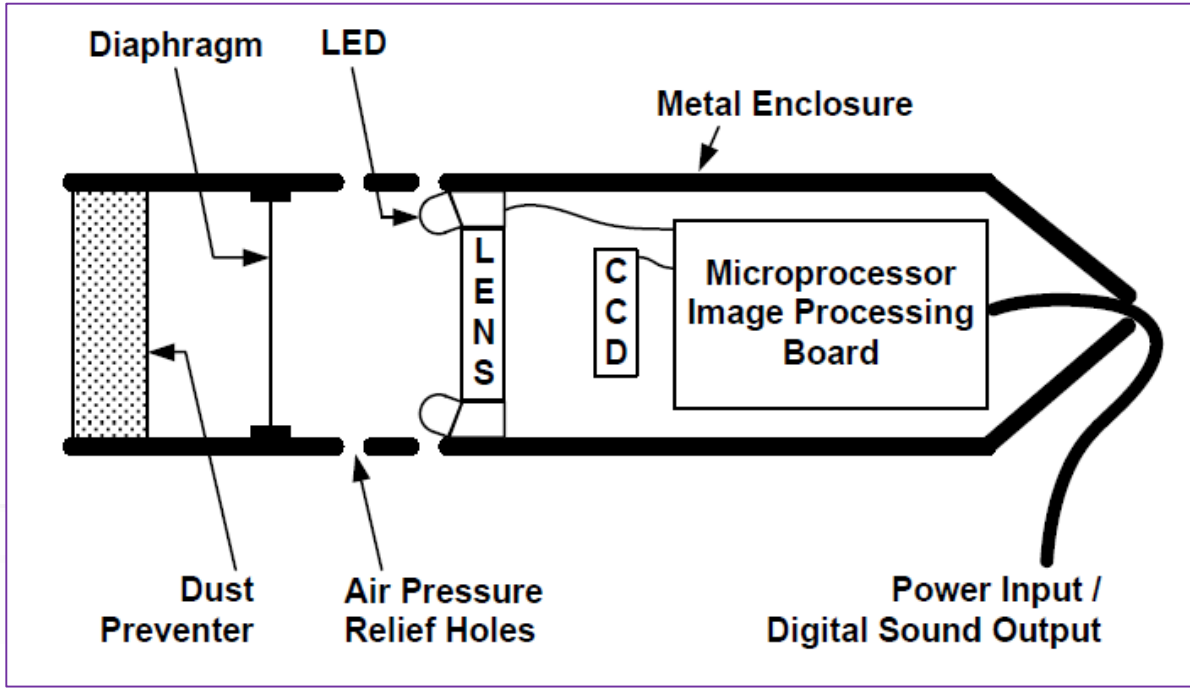

Comparison of the new microphone to the other known types of optical microphones

	Cost of Technology	Dynamic Range	Demonstrated Frequency Response Range	Total Harmonic Distortion
New microphone	Very low	20–140 dB SPL	20 Hz–16,000 Hz	Low (< 1%)
Interferometry-based microphones	High	30–120 dB SPL	20 Hz–20,000 Hz	Low (< 1%)
Light intensity-based microphones	Low	30–120 dB SPL	20 Hz–8,000 Hz	Low (< 1%)

Theory

The instantaneous displacement of the diaphragm:

The vibrating metallic diaphragm in the present microphone can be modeled as a forced harmonic oscillator

The standard solution of the problem of the forced harmonic oscillator gives the instantaneous displacement **x(t) of the oscillator as**

$$x(t) = \frac{F_{max}\sin(\omega t + \phi)}{m\sqrt{(\omega_0^2 - \omega^2)^2 + \beta^2\omega^2}}$$

where m is the mass of the oscillator (the diaphragm),

$\omega_0 = \sqrt{k/m}$ is the natural frequency of oscillation,

ϕ is the possible phase shift

k is the spring constant

β is the damping constant

$F_{max}\sin\omega t$ is the sinusoidal force acting on the oscillator

Theory

The force that is acting on the diaphragm is equal to the acoustic pressure P multiplied by the surface area A of the diaphragm, hence

$$x(t) = \frac{A}{m\sqrt{(\omega_0^2 - \omega^2)^2 + \beta^2\omega^2}} P_{max} \sin(\omega t + \phi)$$

two unknown constants in Eq are the natural frequencyw_0 and the damping constant β

By knowledge of w_0, β can be determined from Eq. (2) if the displacement $x(t)$ is simply measured at the natural frequency; that is, if w =w_0,

$$\beta = \frac{A/m}{x_{max}\omega_0} P_{max}$$

and hence β can be determined by measuring the maximum displacement x_{max} for a certain applied acoustic pressure P_{max}

Theory

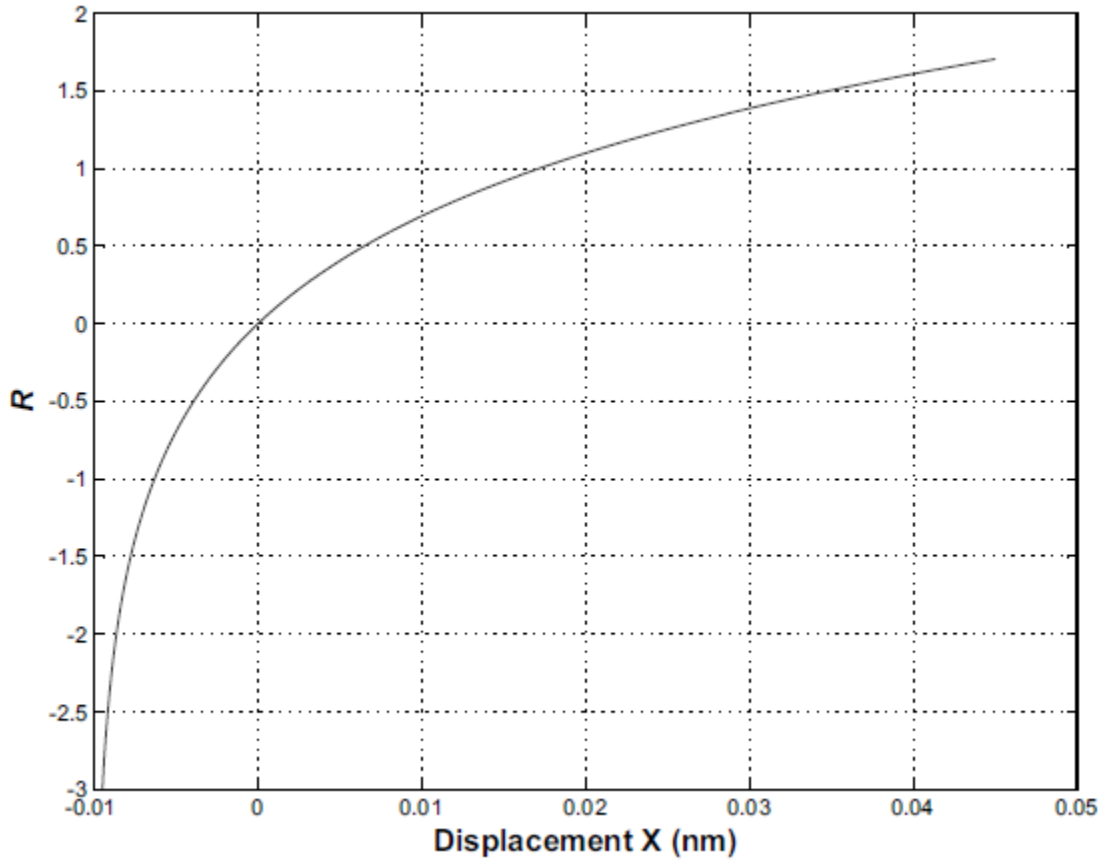

Recognition function *R* vs. diaphragm displacement in nm

Theory

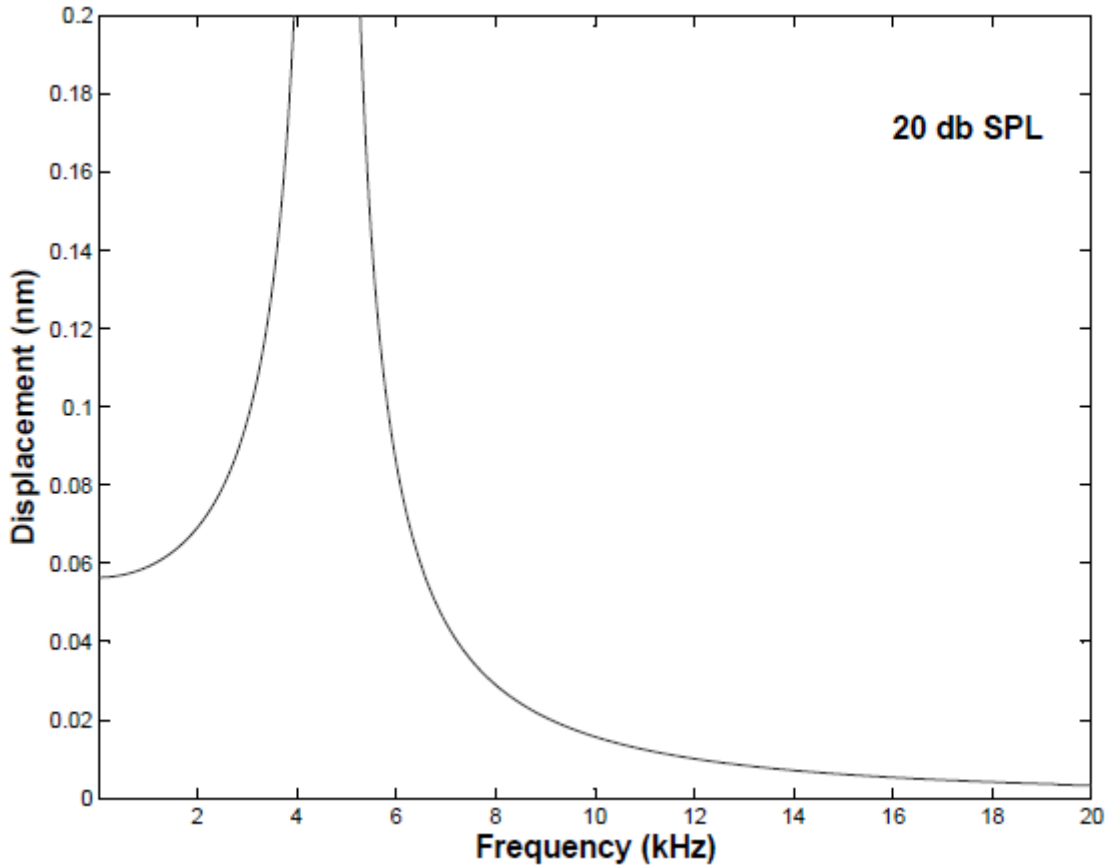

Maximum displacement of the diaphragm vs. frequency at a sound pressure of 20 db SPL.

Theory

Flowchart of the code used
in conjunction with the image processing board.

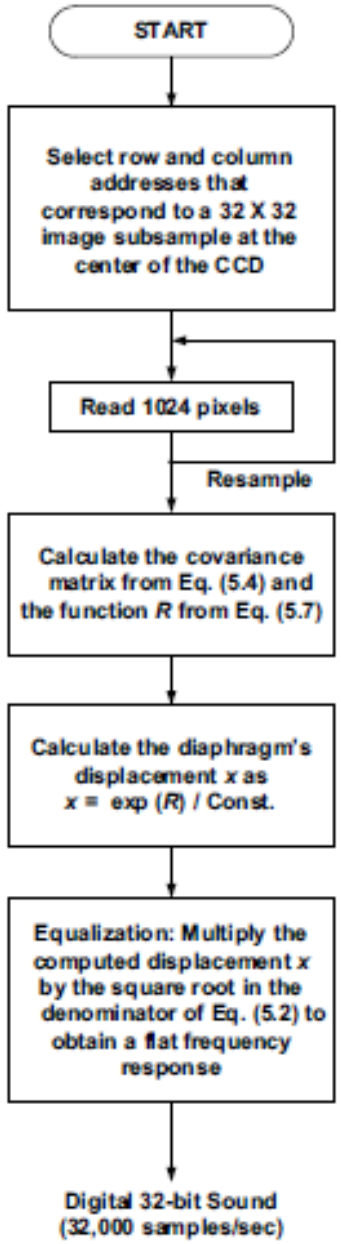

Unit-step function response of the diaphragm.

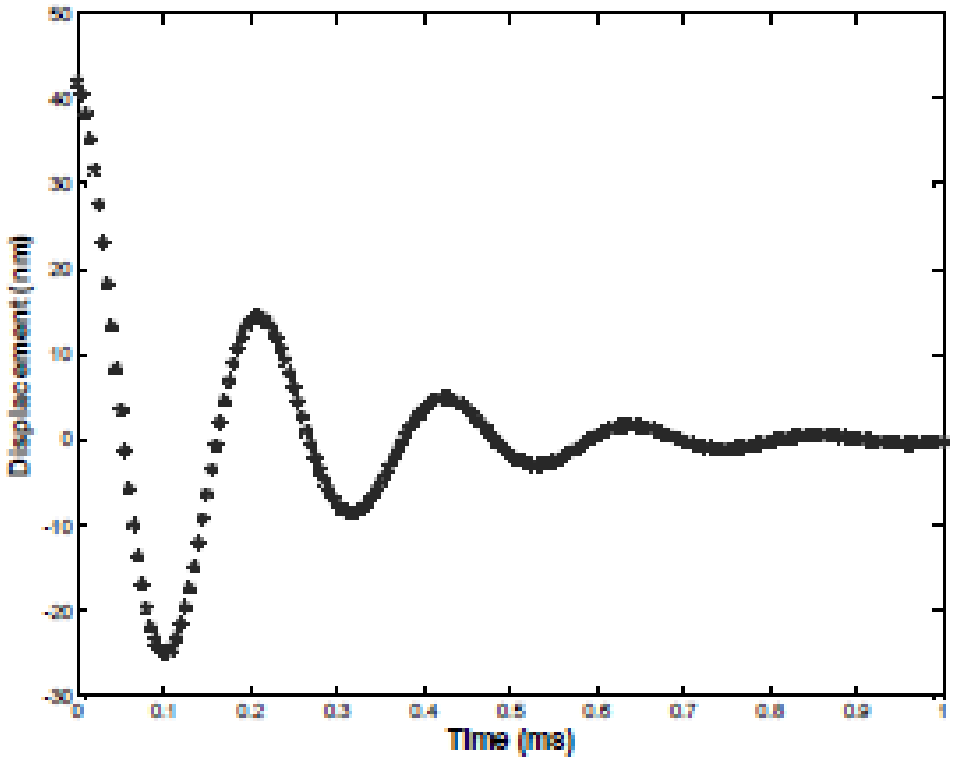

Probability of error as a function of the image size at 20 db SPL.

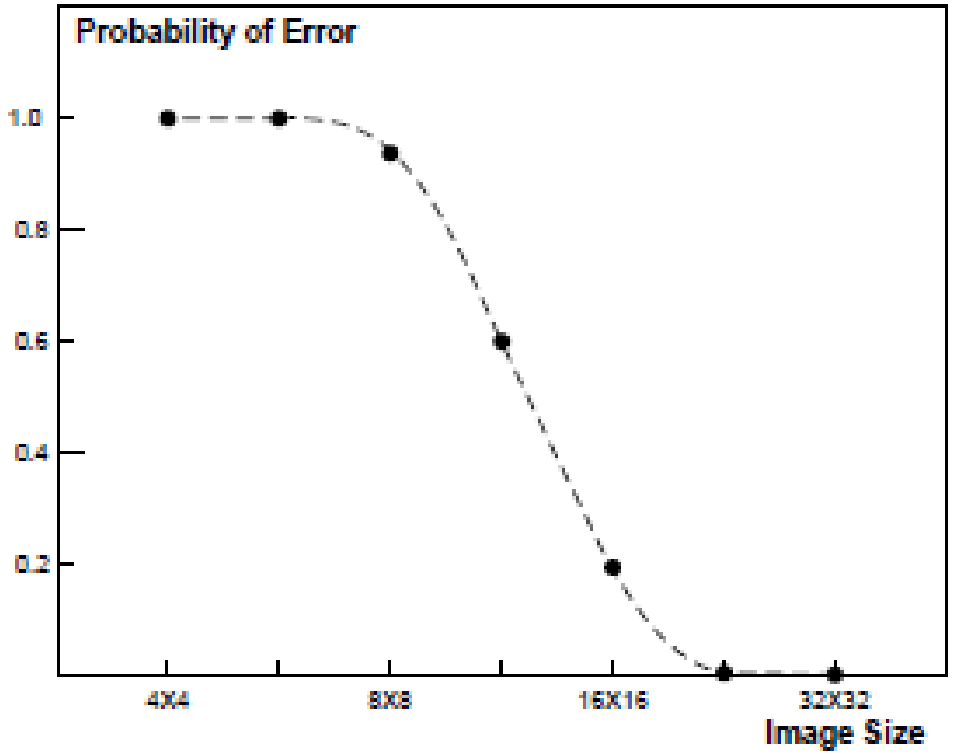

Conclusion

The new optical microphone introduced in this section features the same excellent qualities of optical acoustic sensors that are based on interferometry, with a much simpler design and at a fraction of the cost. Based on pattern recognition principles and highly integrated, high-speed electronics, the microphone captures image samples at a rate of 32 kHz and estimates the instantaneous displacement of the diaphragm from each sample

Other Optoelectronic and Photonic Micro Sensors

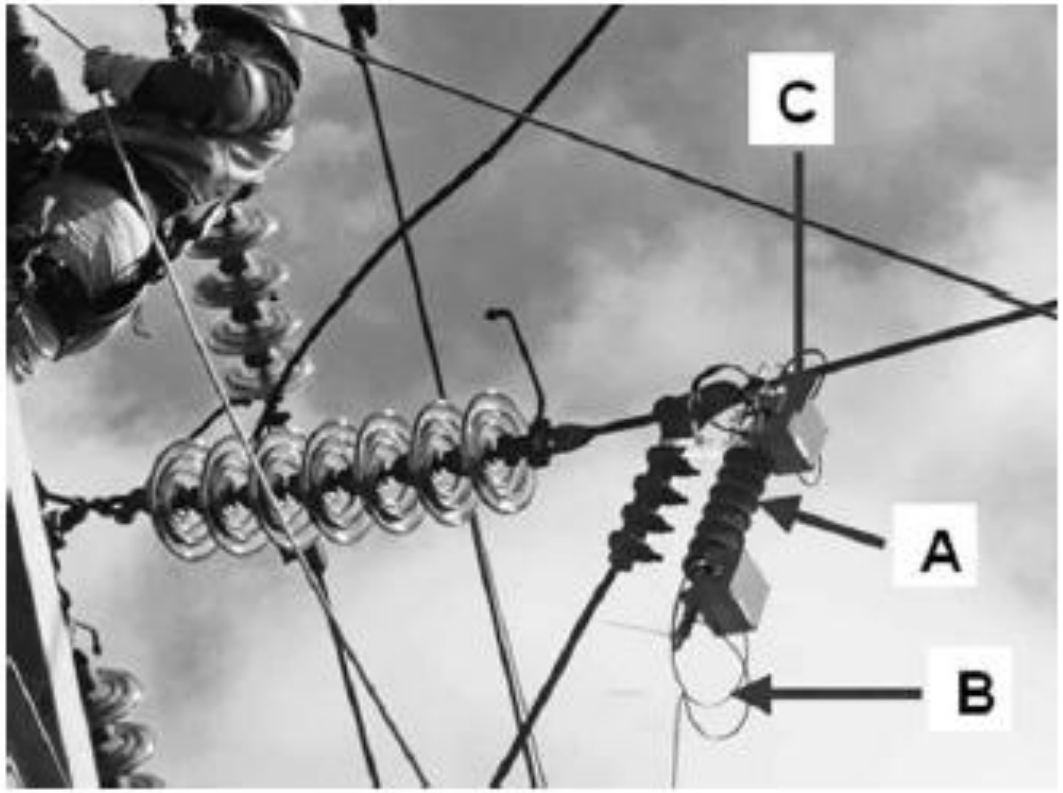

Hybrid optoelectronic sensor for current and temperature monitoring in overhead transmission lines